Geochemistry Geophysics Geosystems G3
AN ELECTRONIC JOURNAL OF THE EARTH SCIENCES
Published by AGU and the Geochemical Society

Article
Volume 7, Number 11
7 November 2006
Q11006, doi:10.1029/2006GC001355
ISSN: 1525-2027

Mechanical limits to microbial activity in deep sediments

Verónica Rebata-Landa and J. Carlos Santamarina
Civil and Environmental Engineering, Georgia Institute of Technology, 790 Atlantic Drive, Atlanta, Georgia 30332-0355, USA (vero@gatech.edu)

[1] The observed decline in microbial abundance with increasing depth has been associated to various environmental factors. Meanwhile, the role of geometrical constraints and soil-bacteria mechanical interactions remains poorly analyzed. Pore and pore-throat sizes may restrict habitable pore space and traversable interconnected porosity, and sediment-cell interaction may cause puncture or tensile failure of the cell membrane. In this study we compile published evidence on the presence of bacteria in deep sediments as well as pore and pore-throat size data in sediments at different depths to establish possible geometrical conditions for the sediment-cell complex. Compiled data are complemented with experimental results gathered through controlled axial compression experiments that reproduce the mechanical consolidation of deep sediment sequences. Then, we analyze the mechanical interaction between bacteria and sediments that may cause cell death. Finally, we combine data and model predictions to define the main regions in a particle-size versus depth space that characterize the fate of bacteria: "active and motile," "trapped inside pores," and "dead or dormant." These regions constrain hypotheses related to the role of biological activity in deep sediments, research protocols and sampling methods, the viability of bioremediation strategies for contaminated sites, and the potential development of bioengineered sediments.

Components: 5876 words, 4 figures, 4 tables, 1 dataset.

Keywords: microorganisms; soils; sediments; porosity; survivability; mechanical stress.

Index Terms: 0416 Biogeosciences: Biogeophysics; 0418 Biogeosciences: Bioremediation.

Received 1 May 2006; **Revised** 20 July 2006; **Accepted** 11 August 2006; **Published** 7 November 2006.

Rebata-Landa, V., and J. C. Santamarina (2006), Mechanical limits to microbial activity in deep sediments, *Geochem. Geophys. Geosyst.*, *7*, Q11006, doi:10.1029/2006GC001355.

1. Introduction

[2] Microorganisms have played a critical role in geological processes leading to the formation of near surface and submerged sediments [*Ehrlich*, 1996; *Hattori*, 1973]. The ubiquitous presence of microorganisms in sediments is presumed and extensively reported in the literature. The observed decline in microbial abundance with increasing depth [*Fierer et al.*, 2003; *Howard-Jones et al.*, 2002; *Kieft et al.*, 1998; *Parkes et al.*, 1994, 2000; *Phelps et al.*, 1994; *Wellsbury et al.*, 2002; *Zhang et al.*, 1998] has been associated to the influence of preferential paths in the transport of microbes through the sediment profile [*Abu-Ashour et al.*, 1994], limited input of fresh organic carbon at the surface and/or use of recalcitrant old buried organic matter by deep bacteria [*Parkes et al.*, 2000; *Wellsbury et al.*, 2002; *Zhang et al.*, 1998], and low hydraulic conductivity or diffusion for the transport of required chemicals [*Fredrickson et al.*, 1991; *Phelps et al.*, 1994].

[3] However, geometrical constraints and mechanical interactions must be considered as well. For example, it has been recognized that small pores restrict bacteria movement and activity [*Fredrickson et al.*, 1997], limit nutrient transport [*Boivin-Jahns et al.*, 1996; *Wellsbury et al.*, 2002], diminish space availability [*Zhang et al.*, 1998], slow the rate of division [*Boivin-Jahns et al.*, 1996], and lead to reduced biodiversity; in fact, spatial isolation due to lack of pore connectivity implies that all cells in a pore are lineal descendants of a bacterium that became entombed at the time of geologic deposition [*Boivin-Jahns et al.*, 1996; *Kieft et al.*, 1998; *Treves et al.*, 2003; *Zhou et al.*, 2002, 2004]. Previous studies suggest that the size of pore throats must be around twice the cell diameter for bacteria transit [*Updegraff*, 1982]. Still, a detailed analysis is lacking.

[4] The goals of this study are to identify geometric restrictions for bioactivity, to develop cell-level mechanical models for bacteria-sediment interaction, and to define regions for bacteria's fate in the two dimensional space of sediment grain size versus burial depth. The scope of this study is limited to microorganisms present in natural and artificially compacted, fracture-free sediments.

2. Materials and Methods

[5] Three approaches are used for this study: data compilation from published studies, experimental study, and analyses based on particle-level geometrical-mechanical models.

2.1. Data Synthesis: Geometric Constraints Represented by Pore and Pore-Throat Sizes

[6] A database of published scanning electron microscopy (SEM) pictures and mercury intrusion porosimetry (MIP) data was compiled to explore the presence of habitable pore space and traversable pore throats in fine-grained sediments subjected to various stress levels. (Note: the term "sediment" is used herein to refer to either residual or transported materials made of mineral grains).

[7] Assuming a nominal 1 μm microbial cell diameter, a sediment is considered to contain habitable pore space if more than 5% of the pores are larger than 1 μm (estimated as area ratio from SEM pictures). On the other hand, a sediment is considered to have traversable pore throats if the probability of having a pore throat larger than 1 μm is higher than 5% (taken as the area ratio under the MIP curve). The particle size and depth corresponding to each data point is extracted from the information provided in the published works. The selected representative particle size is the 10th percentile d_{10} because the finer fraction that fills the voids between large particles determines the hydraulic conductivity, porosity, pore size distribution and therefore the effective pore size in the sediment mass. In the case of laboratory studies, depth is computed from the applied effective overburden stress.

2.2. Data Synthesis: Bacteria in Sediments

[8] The second database that is compiled consists of reported cases of "viable" bacteria in sediments. Each entry in the database includes the representative particle size d_{10} and the corresponding depth. We carefully analyzed each case history; still, there may be biases in the database related to contamination and sampling effects [*Boivin-Jahns et al.*, 1996], reactivation of dormant cells during core extraction [*Zweifel and Hagstrom*, 1995], cell growth during storage [*Sinclair et al.*, 1990] and our interpretation of particle size when authors provide descriptive information only.

2.3. Experimental Study

[9] One-dimensional compression tests were used to explore the d_{10} versus depth space where biological evidence is insufficient. The following sediments, cells and devices were used.

2.3.1. Sediments

[10] Five sediments were chosen for their particle size, compatible solution pH and grain strength characteristics: Crushed silica flour (Sil-co-sil, d_{10} = 10 μm), Precipitated silica flour (Zeo; d_{10} = 20 μm uncrushed; 0.1 μm after crushing), Kaolinite (RP2, d_{10} = 0.36 μm), Illite (IMt-1, d_{10} = 0.04 μm), and Montmorillonite (Bent, d_{10} = 0.0034 μm).

2.3.2. Bacterial Species

[11] The selected strain is *Pseudomonas fluorescens*; this is a mesophilic, non-spore-forming species naturally present in sediments.

2.3.3. Test Device

[12] The system consists of a set of six stainless steel one-dimensional compression chambers which are loaded using pneumatic cylinders. The air pressure control permits applying preselected effective overburden stress levels between 30 kPa and 9 MPa (i.e., ~3 m to ~900 m burial depth).

Table 1. Specimen Preparation

Sediment Type	Sterile Sediment Mass, g	Culture Volume, mL	Sterile Nutrient Volume, mL
Crushed silica flour	1.0	2.0	2.0
Precipitated silica flour	1.0	2.0	2.0
Kaolinite	4.0	1.5	1.5
Illite	4.0	2.0	2.0
Montmorillonite	1.0	3.0	3.0

2.3.4. Other Materials

[13] The nutrients are Difco Nutrient Broth for pore fluid, and Difco Nutrient Agar for Petri plates (Fisher Scientific). Sterile hydrophilic microfilter discs (13 mm diameter, 0.2 μm filtration - Fisher Scientific) were used at both ends of the specimen to facilitate drainage during consolidation and to prevent external contamination.

2.3.5. Test Procedures

[14] All procedures were conducted under aseptic conditions. Sediments, broth, agar and all device parts in contact with the sediment (piston, chamber and base) were autoclaved at 124°C and 125 kPa for 35 min. Sediments and broth were stored at 3°C in sterile containers, while agar was poured into Petri plates and stored at 3°C. Frozen cells were transferred into sterile Petri plates containing agar and incubated 24 hours at the optimum growth temperature (25°C for *Pseudomonas fluorescens*). Then, a 24 hours colony was transferred into 5 mL sterile broth, shaken thoroughly and incubated for additional 24 hours at the optimum growth temperature. A total of six 5 mL vials were prepared following this procedure (one per chamber). Prior analyses demonstrated that this procedure produces $\sim 10^8$ cells/mL.

[15] Prior to assemblage, device parts were rinsed thoroughly with alcohol. The microfilter disc was placed on the base and the testing chamber was set in place. Half of the sterile sediment was transferred aseptically inside the chamber, culture from the vials and sterile broth were added and mixed with the sediment; then, the rest of the sediment was incorporated and mixed until a uniform paste was obtained. The amounts of sediment, culture and nutrient vary with sediment type (to achieve saturation) and are shown in Table 1.

[16] Finally, a second microfilter disc was placed on top of the sediment and pushed slightly using the piston. Thereafter, pistons were step loaded until the target effective overburden stress was reached. The load was sustained during 48 to 72 hours. Longer loading periods were avoided to minimize the effects of nutrient deficit and waste accumulation on bacterial survivability.

[17] Finally, the chamber was disassembled to recover the sediment specimen. The periphery of each specimen was aseptically trimmed to reduce the probability of contamination, and approximately 0.5 mL of each specimen was introduced into vials, prepared with 4.5 mL Phosphate Buffered Saline (PBS) solution. Vials were sonicated for 10 to 20 seconds to detach cells from sediment particles and 0.1 mL of the fluid was transferred into agar plates, spread using a sterile tool and incubated for 24 hours at the optimum temperature.

[18] This protocol was designed to prevent contamination. The adequacy of the procedure was corroborated by sterile controls run for all sediments and stress combinations. Furthermore, the complete study was duplicated for verification, obtaining identical results.

2.4. Particle-Level Analytical Models

[19] Various geometrical and mechanical interaction models were analyzed to establish boundaries and the effect of effective overburden stress and particle size on bacteria's fate. All models assume initial spherical cell shape, constant cell volume and constant cell wall volume and are available as Electronic Supplements[1]. Relevant geometrical and mechanical properties used in the models are summarized in Table 2. Brief comments on each of the models follow (equations in Table 3).

2.4.1. Habitable Pore Space and Traversable Pore Throats (Table 3, Models a and b)

[20] Cells can loosely fit inside pore spaces without suffering mechanical stresses when $d_{cell} \ll d_{pore}$. For cubic-tetrahedral and simple cubic packing of

[1] Auxiliary materials are available in the HTML. doi:10.1029/2006GC001355.

Table 2. Mechanical and Geometrical Properties of Bacteria[a]

Property	Average Value	References
Cell wall elastic modulus, E_{cell}	30 MPa	*Boulbitch et al.* [2000]; *Thwaites and Surana* [1991]; *Yao et al.* [1999]
Cell wall tensile strength, σ_t	13 MPa	*Thwaites and Surana* [1991]; *Thwaites et al.* [1991]
Drag velocity of cells, v	10 μm/s	*Astumian and Hanggi* [2002]
Cell radius, R	0.5 μm	*Katz et al.* [2003]
Cell wall thickness, t	50 nm	*Edwards* [1990]

[a] Note: Average values for bacteria commonly found in sediments.

monosized spherical particles size $d_{sediment}$, the pore size varies from $d_{pore} = 0.26\ d_{sediment}$ to $0.37\ d_{sediment}$.

2.4.2. Cell Squeezed Between Two Particles (Table 3, Model c)

[21] Large platy particles such as kaolinite can be as large as or larger than the cell size. The loading mechanism resembles a sphere being squeezed between two large plates. The deformed cell gains a filled torous shape until the cell wall fails in tension.

2.4.3. Cell Puncture (Table 3, Model d)

[22] The thickness of kaolinite and illite clay particles are one or two orders of magnitude smaller than cells, and therefore the loading mechanism resembles a spherical bacteria being ''pressed by needles'' until they eventually puncture the cell [*Sun et al.*, 2003]. The lower limit for this model corresponds to the smallest particle that can exert the required puncture force without buckling, i.e., when platy sediment particles experience excessive bending before perforating the cell wall.

2.4.4. Cell Squeezed Within the Equivalent Continuum Sediment Skeleton (Table 3, Model e)

[23] When sediment particles are much smaller than the cell, e.g., montmorillonite, the cell is effectively submerged in an equivalent continuum, and sediment particles are not strong enough to puncture the cell wall. However, as the burial depth of the sediment increases, particles move closer together by compression of the counterion diffuse layer, reducing the space around the cell. In this case a trapped cell can be axially deformed into a filled torous until its cell wall breaks in tension. For this model, the initial interparticle distance is assumed to be equal to twice the diffuse layer thickness and the limit deformation is established at an interparticle distance of 10 Å. According to this mechanical model and the parameters summarized in Table 3, reversed arching takes place within the sediment skeleton and the cell takes more load than the neighboring particles due to the high sediment skeleton compliance. The position of this boundary depends on the lateral effective stress, which is linked to the sediment formation history. Nutrient and waste transport are slow in these fine-grained sediments and may become the limiting factor.

2.4.5. Cell Entrapment and Mobilization Inside the Sediment Skeleton (Table 3, Model f)

[24] Motile microbial cells can generate a viscous drag force in the order of 0.1-to-10 pN [*Astumian and Hanggi*, 2002; *Miyata et al.*, 2002]. This force may be sufficient to displace neighboring particles. The boundary for this mechanism in the d_{10} versus depth space is computed with the displacement model presented in Table 3 (Model f), which considers the particles self weight and the skeletal force per particle, and disregards electrostatic interactions between cells and fine-grained sediment particles. Note that the model considers the displacement of a single particle rather than the area corresponding to the cell's cross section.

3. Results

[25] Results from the data synthesis exercise, the experimental study, and computed with analytical models are presented in the same two dimensional space defined by particle size and equivalent burial depth (which is a surrogate for effective overburden stress level), to identify boundaries for the mechanical limits of microbial activity in deep sediments.

3.1. Data Synthesis: Geometric Constraints

[26] Habitable pore space and traversable pore-throat sizes for a 1 μm nominal bacteria size are shown in Figure 1. The data show that habitable pores and traversable pore throats are found in

Table 3. Models for Bacteria-Sediment Mechanical Interaction[a]

Model	Relevant Equations	Particle Size Range
(a) Habitable pore	$R_{throat} = t_p \cdot \left(\frac{\sqrt{3}}{3} - \frac{1}{2}\right) \approx 0.08 \cdot t_p$	silts and sands
	$R_{pore} = t_p \cdot \left(\frac{\sqrt{21}}{6} - \frac{1}{2}\right) \approx 0.26 \cdot t_p$	
(b) Traversable pore throats	$R_{throat} = t_p \cdot \left(\frac{\sqrt{2}}{2} - \frac{1}{2}\right) \approx 0.21 \cdot t_p$	silts and sands
	$R_{pore} = t_p \cdot \left(\frac{\sqrt{3}}{2} - \frac{1}{2}\right) \approx 0.37 \cdot t_p$	
(c) Squeezing	$H_{\max} = \frac{E_{cell}}{\gamma_{eff}} \cdot \frac{9}{\pi} \cdot \frac{\alpha \cdot \varphi \cdot (1 - 2 \cdot \varphi)}{\frac{\pi}{7} - \frac{1}{2} \cdot \varphi} \cdot \left(\frac{\varphi^{1/3}}{1 - \varphi^{1/3}}\right)^2$	$t_p \geq t_{p\_critic}$
		$t_{p\_critic} = \frac{6 \cdot R}{\pi} \cdot \left(\frac{\varphi^{1/3}}{1 - \varphi^{1/3}}\right)$
(d) Puncture	$H_{\max} = \frac{81}{4 \cdot \pi} \cdot \frac{E_{cell}}{\gamma_{eff}} \cdot \alpha \cdot \psi \cdot \varphi^{5/2}$	$t_{p\_buckling} < t_p < t_{p\_critic}$
		$t_{p\_buckling} \approx 125 \cdot \frac{E_{cell}}{E_{soil}} \cdot \alpha \cdot R \cdot \varphi^{5/2}$
(e) Equivalent continuum	$H_{\max} = \mathrm{B} \cdot \left(\frac{2 \cdot \pi^2}{\left(2 - \varphi^{1/3} + \frac{1}{2} \cdot \varphi^{1/3} \cdot \frac{t_p}{\xi}\right)^2} - 1\right) + \frac{E_{cell}}{\gamma_{eff}} \cdot \frac{9}{16 \cdot \pi} \cdot \frac{\alpha \cdot \varphi \cdot (1 - 2 \cdot \varphi)}{\frac{\pi}{7} - \frac{1}{2} \cdot \frac{\varphi}{(1 - K_0)^3}} \cdot \left(\frac{\frac{\varphi^{1/3}}{1 - K_0}}{1 - \frac{\varphi^{1/3}}{1 - K_0}}\right)^2$	$t_p \leq \left(\frac{4}{\varphi^{1/3}} - 2\right) \cdot \xi$
	$\mathrm{B} = \frac{R_{gas} \cdot T \cdot c_0}{2 \cdot \gamma_{eff}} \qquad \xi = \sqrt{\frac{\varepsilon_0 \cdot R_{gas} \cdot \kappa \cdot T}{2 \cdot F_a^2 \cdot c_0 \cdot z^2}}$	
(f) Single particle displacement	$H_{pushing} = \frac{6 \cdot \pi \cdot \eta \cdot v}{R \cdot \psi^2 \cdot \mu \cdot \gamma_{eff}}$	$t_p \leq t_{p\_max\ imum}$
		$t_{p\_max\ imum} = \sqrt{\frac{36 \cdot \eta \cdot v \cdot R}{\gamma_{grains} - \gamma_w}}$

[a] Notation: $\alpha = \frac{t}{R}$, where t is initial cell wall thickness and R is initial cell radius; $\psi = \frac{t_p}{R}$, where t_p is particle thickness and R is initial cell radius; $\varphi = \frac{\sigma_{tensile}}{E_{cell}}$, where $\sigma_{tensile}$ is cell wall tensile strength and E_{cell} is cell wall elastic modulus. R_{pore} and R_{throat}, radius of pore and pore throat for a given geometric configuration; $H_{\max}$, maximum depth before the cell wall fails; $H_{pushing}$, maximum depth where cell can push sediment particles; R_{gas} = 8.314 N-m/°K-mol; T, absolute temperature; c_0 [mol/m^3]; ξ, double layer thickness; permittivity of free space $\varepsilon_0 = 8.85 \times 10^{-12}$ F/m; real relative permittivity of water κ = 78.5; Faraday's constant $F_a = 9.6485 \times 10^4$ C/mol; z, valence of cations; E_{cell}, elastic modulus of cell wall; γ_{eff}, effective unit weight of sediment mass; K_0, lateral stress coefficient; E_{soil}, elastic modulus of sediment particle; R, radius of bacterial cell; v, velocity of bacterial cell; η, viscosity of pore fluid; μ, friction coefficient; t_p, particle size. For Figure 3, γ_{eff} = 10 kN/m^3, K_0 = 0.2, E_{soil} = 5 GPa, $\eta = 1 \times 10^{-6}$ g/μm-s, and and μ = 0.5.

Geochemistry Geophysics Geosystems G3
REBATA-LANDA AND SANTAMARINA: MICROBES
10.1029/2006GC001355

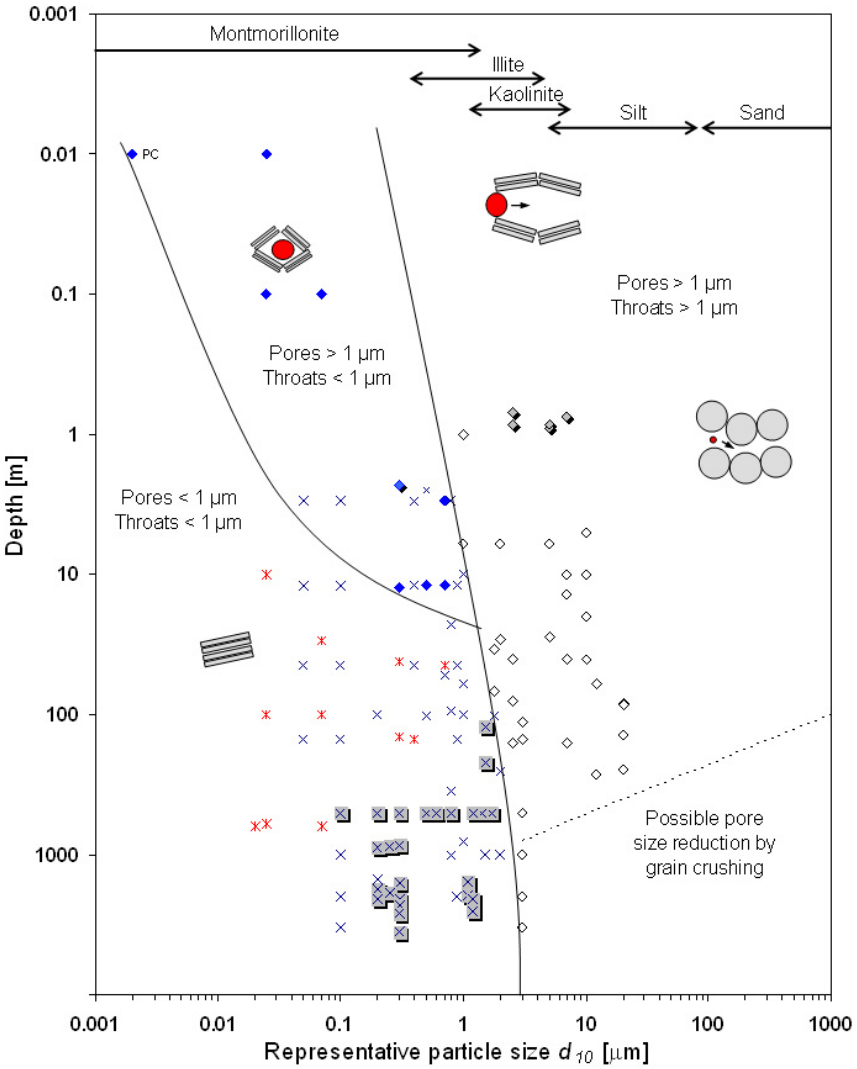

Figure 1. Pore and pore-throat size. Habitable pore space (solid diamonds) (SEM), traversable pore throat (open diamonds) (MIP), nonhabitable pore space (asterisks) (SEM), and nontraversable pore throat (crosses) (MIP). Lines suggest estimated limits for each geometric configuration. MIP data from *Ahmed et al.* [1974], *AlMukhtar et al.* [1996], *Bolton et al.* [2000], *Cuisinier and Laloui* [2004], *Delage and Lefebvre* [1984], *Delage et al.* [1996], *Dewhurst et al.* [1998, 1999], *Diamond* [1971], *Garcia-Bengochea et al.* [1979], *Griffiths and Joshi* [1989, 1990], *Heling* [1970], *Horsrud et al.* [1998], *Juang and Holtz* [1986], *Lapierre et al.* [1990], *Lohnes et al.* [1976], *Penumadu and Dean* [2000], *Simms and Yanful* [2001, 2004], *Sridharan and Altschaeffl* [1971], *Tanaka et al.* [2003], *Vasseur et al.* [1995], and *Yang and Aplin* [1998]. SEM pictures from *Delage and Lefebvre* [1984], *Griffiths and Joshi* [1990], *Hicher et al.* [2000], and *Negre et al.* [2004]. Underlined data labels indicate natural samples; all other data points were obtained from artificially compacted specimens (PC: personal communication, M. Santagata, 2005). Typical mineral sizes are indicated in the upper part of the plot [*Mitchell*, 1993; *Santamarina et al.*, 2001].

coarse sediments, and in some clayey sediments at shallow depth.

[27] Silt and sand grains may crush at large burial depths and cause a reduction in pore and pore-throat sizes. The depth required for crushing is inversely proportional to the particle diameter and directly proportional to the tensile strength of the mineral that makes the grains [*McDowell and Bolton*, 1998]. The dotted line in Figure 1 captures the estimated grain crushing boundary.

[28] Data in Figure 1 provides a geometric explanation for the generally observed decrease in microbial abundance with decreasing particle size [*Fredrickson et al.*, 1991; *Phelps et al.*, 1994;

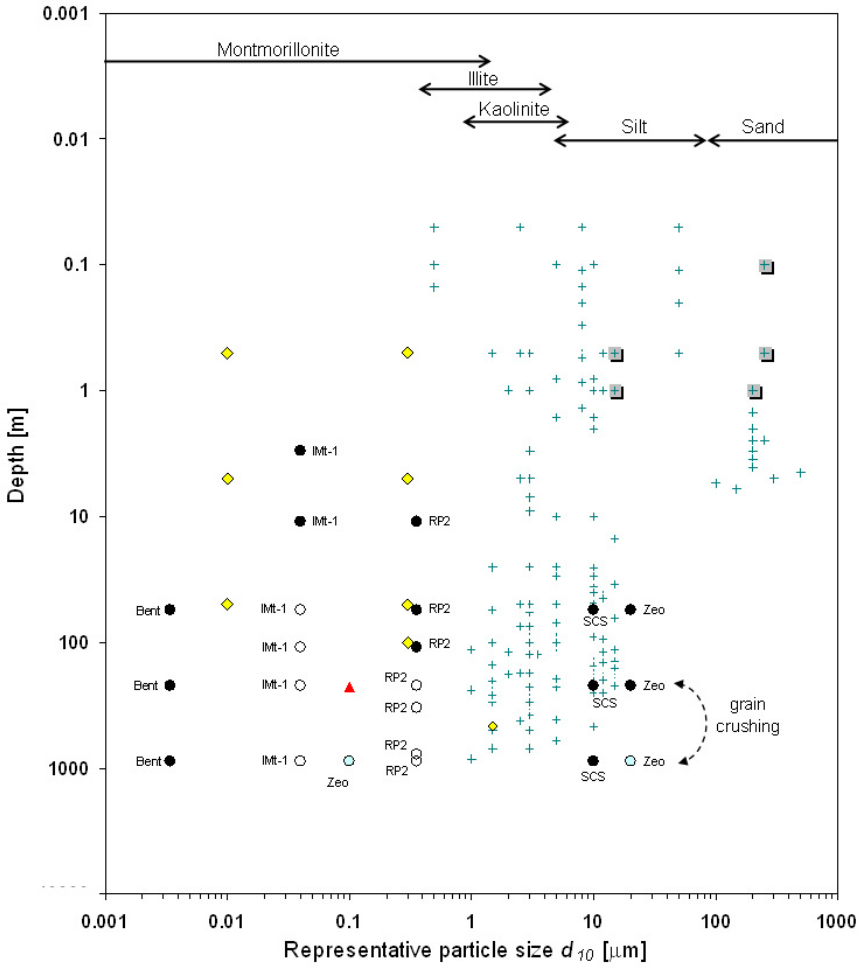

Figure 2. Presence of bacteria in sediments [*Agnelli et al.*, 2004; *Bird et al.*, 2001; *Blume et al.*, 2002; *Boivin-Jahns et al.*, 1996; *Chen et al.*, 2003; *Cragg et al.*, 1996; *D'Hondt et al.*, 2004; *Dodds et al.*, 1996; *Fierer et al.*, 2003; *Fredrickson et al.*, 1991; *Phelps et al.*, 1994; *Sinclair and Ghiorse*, 1989; *Sinclair et al.*, 1990; *Wellsbury et al.*, 1996, 2002; *Zhang et al.*, 1998]. Detected bacteria (crosses), reduced diversity–nondividing cells (open diamonds), possible contamination (triangle) (as reported by the authors). Lack of reported data in certain regions does not imply impossible living conditions. Experimental data gathered in this study: solid circles, alive; open circles, dead. Underlined data labels correspond to unsaturated sediment specimens. Data from *Agnelli et al.* [2004], *Blume et al.* [2002], *Chen et al.* [2003], *Dodds et al.* [1996], *Fierer et al.* [2003], and *Sinclair and Ghiorse* [1989] do not specify water saturation conditions; the remaining data correspond to presumably saturated sediments. Dashed curved arrow indicates negative plates in precipitated silica flour after grain crushing at high overburden stresses which causes a particle size reduction from ~20 μm to ~0.1 μm.

Sinclair et al., 1990; *Zhang et al.*, 1998], and the comparatively low microbial diversity found in deep, fine-grained sediments [*Marchesi et al.*, 2001; *Newberry et al.*, 2004; *Zhou et al.*, 2004]. Both can be linked to lack of habitable pore space and hindered mobility across pores.

3.2. Data Synthesis: Presence of Bacteria in Sediments

[29] The compiled data shown in Figure 2 emphasize the presence of bacteria in sediments with representative grain size $d_{10} > 1$ μm. Reduced biodiversity is reported in various cases that either involve sediments with $d_{10} < 1$ μm or high burial depth. Positive reports are predominant for silts and sands. In contrast, there is limited data for finer sediments, and contamination is suspected in some cases (as reported by some of authors). It is important to note that bioactivity at depth may be restricted by other limiting factors such as lack of nutrients. Therefore published data (in the absence of contamination) should be considered as one-way indicators: documented bioactivity suggests that proper conditions exist; however, the absence of

Table 4. Colony-Forming Units per mL of Sediment (CFU/mL-Sediment) in Recovered Specimens

Equivalent Depth, m	Bentonite (Bent)	Illite (IMt-1)	Kaolinite (RP2)	Crushed Silica Flour (Sil-co-sil)	Precipitated Silica Flour (Zeo)
3.0		$>10^5$			
11.0		$>10^5$	$>10^5$		
55.2	$>10^5$	**0**	$>10^5$	12×10^3	$>10^5$
110.3		**0**	8×10^3		
220.6	5×10^3	**0**	**0**	6×10^3	$>10^5$
330.9			**0**		*(crushing)*
772.2			**0**		
882.5	2×10^3	**0**	**0**	5×10^3	**0**

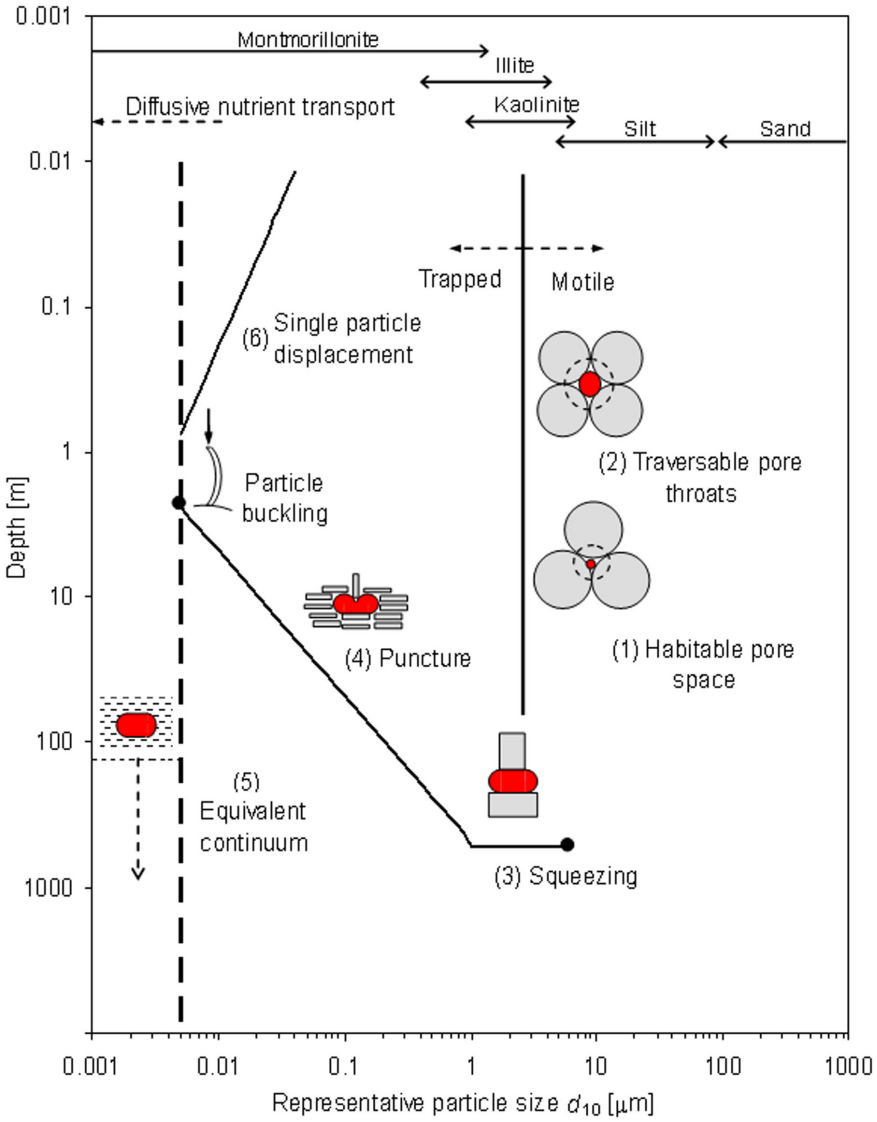

Figure 3. Sediment-bacteria mechanical interaction: predicted boundaries. Parameters and equations are listed in Tables 2 and 3. The position of the equivalent continuum boundary depends on lateral stress; the dashed line shows the shallowest case which corresponds to zero lateral stress.

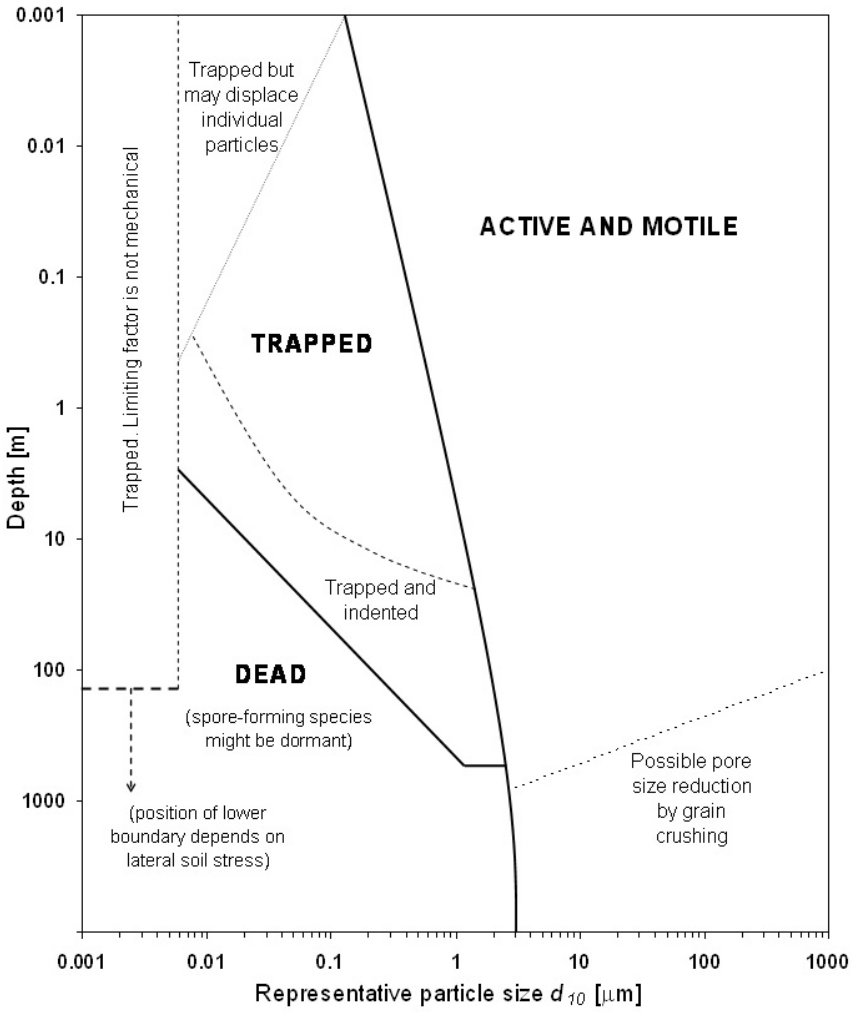

Figure 4. Bacteria's fate in sediments. Regions are defined by combining compiled evidence, new experimental data gathered in this study, pore and pore-throat data, and predicted bacteria-sediment mechanical interactions.

bioactivity does not necessarily imply geometric/mechanical limiting conditions.

3.3. Experimental Results

[30] The experimental study conducted to gather data for sediments and depths that are poorly constrained by the available field data was designed to provide either of two possible outcomes: "dead" when no colonies formed in culture plates after 24 hours, or "alive" when colonies were present in culture plates after 24 hours. Results are superimposed on Figure 2. Average plate counts for each sediment-stress pair are listed in Table 4.

3.4. Model Predictions

[31] Bacteria-sediment interaction models are plotted in Figure 3 in the two dimensional space defined by effective overburden stress and particle size, in terms of depth and d_{10}. These boundaries define different regions for bacteria's fate in sediments. Puncture appears as the most critical mechanism affecting the survivability of bacteria in clayey sediments. Possible variations in cell size, wall thickness and tensile strength have a small effect on the position of the boundaries when they are plotted in the large variable range captured in Figure 3.

4. Discussion

4.1. Combined Effect of Geometric Constraints and Mechanical Interactions

[32] Pore and pore-throat sizes correlate with grain size in silts and sands, where fabric formation is controlled by the particle self-weight and remain

quite stable with stress changes. However, fabric formation is determined by electrostatic interactions in fine-grained clayey sediments, and the sediment structure experiences significant volumetric changes with increasing confinement [*Bennett et al.*, 1991; *Mitchell*, 1993; *Santamarina et al.*, 2001]. Note that pores in clayey sediments can be several times larger than the particles themselves, yet, relatively enclosed.

4.2. Regions for Bioactivity

[33] Geometrical constraints and mechanical interactions suggest different regions for bacteria's fate, identified in Figure 4. (1) "Active and motile" when pore and pore throats are large so that cells can move through the pore network and find sufficient space for growth and metabolic activity. (2) "Trapped inside pores" when pore throats hinder migration; this zone can be subdivided into three subzones depending on the bacteria's ability to push particles and the size of the habitable pore space. (3) "Dead" when burial depths exceed the puncturing and/or squeezing thresholds; spore-forming species may remain dormant, as illustrated in Figure 4. Bacteria in the region that corresponds to very small particle sizes, beyond the buckling limit, may not be mechanically compromised, yet their survivability will be limited by nutrient and waste transport. The geometrical and mechanical constraints to microbial activity identified in Figure 4 apply to fracture-free sediments; the pore size distribution and inter-particle forces in the gauge material within fractures may deviate from those imposed by lithostatic stresses assumed in this study.

4.3. Summary

[34] The extensive biological activity observed in the near-surface cannot be presumed a priori in deep sediments. Pore and pore-throat sizes restrict habitable pore space and traversable interconnected porosity. Furthermore, sediment-cell interaction may cause puncture or tensile failure of the cell membrane. These results restrict the range of grain size and burial depth where biomediated geochemical processes can be expected in sediments, affect the interpretation of geological processes and the development of engineering solutions such as bioremediation.

Acknowledgments

[35] Support for this research was provided by The National Science Foundation and The Goizueta Foundation. The authors are grateful to the reviewers for their insightful observations.

References

Abu-Ashour, J., D. M. Joy, H. Lee, H. R. Whiteley, and S. Zelin (1994), Transport of microorganisms through soil, *Water Air Soil Pollut.*, *75*(1–2), 141–158.

Agnelli, A., J. Ascher, G. Corti, M. T. Ceccherini, P. Nannipieri, and G. Pietramellara (2004), Distribution of microbial communities in a forest soil profile investigated by microbial biomass, soil respiration and DGGE of total and extracellular DNA, *Soil Biol. Biochem.*, *36*(5), 859–868.

Ahmed, S., C. W. Lovell, and S. Diamond (1974), Pore sizes and strength of compacted clay, *J. Geotech. Eng. Div. Am. Soc. Civ. Eng.*, *GT4*, 407–425.

AlMukhtar, M., N. Belanteur, D. Tessier, and S. K. Vanapalli (1996), The fabric of a clay soil under controlled mechanical and hydraulic stress states, *Appl. Clay Sci.*, *11*(2–4), 99–115.

Astumian, R. D., and P. Hanggi (2002), Brownian motors, *Phys. Today*, *55*(11), 33–39.

Bennett, R. H., W. R. Bryant, and M. H. Hulbert (1991), *The Microstructure of Fine-Grained Sediments, From Mud to Shale*, vol. xxii, 582 pp., Springer, New York.

Bird, D. F., S. K. Juniper, M. Ricciardi-Rigault, P. Martineu, Y. T. Prairie, and S. E. Calvert (2001), Subsurface viruses and bacteria in Holocene/Late Pleistocene sediments of Saanich Inlet, BC: ODP Holes 1033B and 1034B, Leg 169S, *Mar. Geol.*, *174*(1–4), 227–239.

Blume, E., M. Bischoff, J. M. Reichert, T. Moorman, A. Konopka, and R. F. Turco (2002), Surface and subsurface microbial biomass, community structure and metabolic activity as a function of soil depth and season, *Appl. Soil Ecol.*, *20*(3), 171–181.

Boivin-Jahns, V., R. Ruimy, A. Bianchi, S. Daumas, and R. Christen (1996), Bacterial diversity in a deep-subsurface clay environment, *Appl. Environ. Microbiol.*, *62*(9), 3405–3412.

Bolton, A. J., A. J. Maltman, and Q. Fisher (2000), Anisotropic permeability and bimodal pore-size distributions of fine-grained marine sediments, *Mar. Petrol. Geol.*, *17*(6), 657–672.

Boulbitch, A., B. Quinn, and D. Pink (2000), Elasticity of the rod-shaped Gram-negative eubacteria, *Phys. Rev. Lett.*, *85*(24), 5246–5249.

Chen, C. R., Z. H. Xu, T. J. Blumfield, and J. M. Hughes (2003), Soil microbial biomass during the early establishment of hoop pine plantation: Seasonal variation and impacts of site preparation, *Forest Ecol. Manage.*, *186*(1–3), 213–225.

Cragg, B. A., R. J. Parkes, J. C. Fry, A. J. Weightman, P. A. Rochelle, and J. R. Maxwell (1996), Bacterial populations and processes in sediments containing gas hydrates (ODP Leg 146: Cascadia Margin), *Earth Planet. Sc. Lett.*, *139*(3–4), 497–507.

Cuisinier, O., and L. Laloui (2004), Fabric evolution during hydromechanical loading of a compacted silt, *Int. J. Numer. Anal. Meteorol.*, *28*(6), 483–499.

Delage, P., and G. Lefebvre (1984), Study of the structure of a sensitive Champlain clay and of its evolution during consolidation, *Can. Geotech. J.*, *21*(1), 21–35.

Delage, P., M. Audiguier, Y. J. Cui, and M. D. Howat (1996), Microstructure of a compacted silt, *Can. Geotech. J.*, *33*(1), 150–158.

Dewhurst, D., A. Aplin, J. Sarda, and Y. Yang (1998), Compaction-driven evolution of porosity and permeability in nat-

ural mudstones: An experimental study, *J. Geophys. Res.*, *103*(B1), 651–661.
Dewhurst, D. N., A. C. Aplin, and J. P. Sarda (1999), Influence of clay fraction on pore-scale properties and hydraulic conductivity of experimentally compacted mudstones, *J. Geophys. Res.*, *104*(B12), 29,261–29,274.
D'Hondt, S., et al. (2004), Distributions of microbial activities in deep subseafloor sediments, *Science*, *306*(5705), 2216–2221.
Diamond, S. (1971), Microstructure and pore structure of impact/compacted clays, *Clay Clay Miner.*, *19*(4), 239–249.
Dodds, W. K., M. K. Banks, C. S. Clenan, C. W. Rice, D. Sotomayor, E. A. Strauss, and W. Yu (1996), Biological properties of soil and subsurface sediments under abandoned pasture and cropland, *Soil Biol. Biochem.*, *28*(7), 837–846.
Edwards, G. (1990), *Biology the Easy Way*, 2nd ed., Barron's Educ. Ser., New York.
Ehrlich, H. L. (1996), *Geomicrobiology*, 3rd ed., vol. xix, 719 pp., CRC Press, Boca Raton, Fla.
Fierer, N., J. P. Schimel, and P. A. Holden (2003), Variations in microbial community composition through two soil depth profiles, *Soil Biol. Biochem.*, *35*(1), 167–176.
Fredrickson, J. K., D. L. Balkwill, J. M. Zachara, S. M. W. Li, F. J. Brockman, and M. A. Simmons (1991), Physiological diversity and distributions of heterotrophic bacteria in deep cretaceous sediments of the Atlantic Coastal Plain, *Appl. Environ. Microbiol.*, *57*(2), 402–411.
Fredrickson, J. K., et al. (1997), Pore-size constraints on the activity and survival of subsurface bacteria in a late Cretaceous shale-sandstone sequence, northwestern New Mexico, *Geomicrobiol. J.*, *14*(3), 183–202.
Garcia-Bengochea, I., C. W. Lovell, and A. G. Altschaeffl (1979), Pore distribution and permeability of silty clays, *J. Geotech. Eng. Div. Am. Soc. Civ. Eng.*, *105*(7), 839–856.
Griffiths, F. J., and R. C. Joshi (1989), Change in pore-size distribution due to consolidation of clays, *Geotechnique*, *39*(1), 159–167.
Griffiths, F. J., and R. C. Joshi (1990), Clay fabric response to consolidation, *Appl. Clay Sci.*, *5*, 37–66.
Hattori, T. (1973), *Microbial Life in the Soil: An Introduction*, vol. vi, 427 pp., CRC Press, Boca Raton, Fla.
Heling, D. (1970), Micro-fabrics of shales and their rearrangement by compaction, *Sedimentology*, *15*(3–4), 247–260.
Hicher, P. Y., H. Wahyudi, and D. Tessier (2000), Microstructural analysis of inherent and induced anisotropy in clay, *Mech. Cohesive Frictional Mater.*, *5*(5), 341–371.
Horsrud, P., E. F. Sonstebo, and R. Boe (1998), Mechanical and petrophysical properties of north sea shales, *Int. J. Rock Mech. Min. Sci.*, *35*(8), 1009–1020.
Howard-Jones, M. H., V. D. Ballard, A. E. Allen, M. E. Frischer, and P. G. Verity (2002), Distribution of bacterial biomass and activity in the marginal ice zone of the central Barents Sea during summer, *J. Mar. Syst.*, *38*(1–2), 77–91.
Juang, C. H., and R. D. Holtz (1986), Fabric, pore-size distribution, and permeability of sandy soils, *J. Geotech. Eng.*, *112*(9), 855–868.
Katz, A., A. Alimova, M. Xu, E. Rudolph, M. K. Shah, H. E. Savage, R. B. Rosen, S. A. McCormick, and R. R. Alfano (2003), Bacteria size determination by elastic light scattering, *IEEE J. Selected Topics in Quantum Electron.*, *9*(2), 277–287.
Kieft, T. L., et al. (1998), Microbial transport, survival, and succession in a sequence of buried sediments, *Microbial Ecol.*, *36*(3), 336–348.
Lapierre, C., S. Leroueil, and J. Locat (1990), Mercury intrusion and permeability of Louiseville clay, *Can. Geotech. J.*, *27*(6), 761–773.
Lohnes, R. A., E. R. Tuncer, and T. Demirel (1976), Pore structure of selected Hawaiian soils, in *Subsidence Over Mines and Caverns, Moisture and Frost Actions, and Classification*, *Trans. Res. Rec. 612*, pp. 76–79, Transp. Res. Board, Washington, D. C.
Marchesi, J. R., A. J. Weightman, B. A. Cragg, R. J. Parkes, and J. C. Fry (2001), Methanogen and bacterial diversity and distribution in deep gas hydrate sediments from the Cascadia Margin as revealed by 16S rRNA molecular analysis, *FEMS Microbiol. Ecol.*, *34*(3), 221–228.
McDowell, G. R., and M. D. Bolton (1998), On the micromechanics of crushable aggregates, *Geotechnique*, *48*(5), 667–679.
Mitchell, J. K. (1993), *Fundamentals of Soil Behavior*, 2nd ed., vol. xiii, 437 pp., John Wiley, Hoboken, N. J.
Miyata, M., W. S. Ryu, and H. C. Berg (2002), Force and velocity of Mycoplasma mobile gliding, *J. Bacteriol.*, *184*(7), 1827–1831.
Negre, M., P. Leone, J. Trichet, C. Defarge, V. Boero, and M. Gennari (2004), Characterization of model soil colloids by cryo-scanning electron microscopy, *Geoderma*, *121*(1–2), 1–16.
Newberry, C. J., G. Webster, B. A. Cragg, R. J. Parkes, A. J. Weightman, and J. C. Fry (2004), Diversity of prokaryotes and methanogenesis in deep subsurface sediments from the Nankai Trough, Ocean Drilling Program Leg 190, *Environ. Microbiol.*, *6*(3), 274–287.
Parkes, R. J., B. A. Cragg, S. J. Bale, J. M. Getliff, K. Goodman, P. A. Rochelle, J. C. Fry, A. J. Weightman, and S. M. Harvey (1994), Deep bacterial biosphere in Pacific Ocean sediments, *Nature*, *371*(6496), 410–413.
Parkes, R. J., B. A. Cragg, and P. Wellsbury (2000), Recent studies on bacterial populations and processes in subseafloor sediments: A review, *Hydrogeol. J*, *8*(1), 11–28.
Penumadu, D., and J. Dean (2000), Compressibility effect in evaluating the pore-size distribution of kaolin clay using mercury intrusion porosimetry, *Can. Geotech. J.*, *37*(2), 393–405.
Phelps, T. J., S. M. Pfiffner, K. A. Sargent, and D. C. White (1994), Factors influencing the abundance and metabolic capacities of microorganisms in eastern coastal-plain sediments, *Microbial Ecol.*, *28*(3), 351–364.
Santamarina, J. C., K. A. Klein, and M. A. Fam (2001), *Soils and Waves: Particulate Materials Behavior, Characterization and Process Monitoring*, vol. xix, 488 pp., John Wiley, Hoboken, N. J.
Simms, P. H., and E. K. Yanful (2001), Measurement and estimation of pore shrinkage and pore distribution in a clayey till during soil-water characteristic curve tests, *Can. Geotech. J.*, *38*(4), 741–754.
Simms, P. H., and E. K. Yanful (2004), A discussion of the application of mercury intrusion porosimetry for the investigation of soils, including an evaluation of its use to estimate volume change in compacted clayey soils, *Geotechnique*, *54*(6), 421–426.
Sinclair, J. L., and W. C. Ghiorse (1989), Distribution of aerobic bacteria, protozoa, algae, and fungi in deep subsurface sediments, *Geomicrobiol. J.*, *7*(1–2), 15–31.
Sinclair, J. L., S. J. Randtke, J. E. Denne, L. R. Hathaway, and W. C. Ghiorse (1990), Survey of microbial populations in buried valley aquifer sediments from northeastern Kansas, *Ground Water*, *28*(3), 369–377.
Sridharan, A., and A. G. Altschaeffl (1971), Pore size distribution studies, *J. Soil Mech. Found. Div. Am. Soc. Civ. Eng.*, *SM5*, 771–787.
Sun, Y., K. T. Wan, K. P. Roberts, J. C. Bischof, and B. J. Nelson (2003), Mechanical property characterization of

mouse zona pellucida, *IEEE Trans. Nanobiosci.*, *2*(4), 279–286.

Tanaka, H., D. R. Shiwakoti, N. Omukai, F. Rito, J. Locat, and M. Tanaka (2003), Pore size distribution of clayey soils measured by mercury intrusion porosimetry and its relation to hydraulic conductivity, *Soils Found.*, *43*(6), 63–73.

Thwaites, J. J., and U. C. Surana (1991), Mechanical properties of Bacillus subtilis cell walls—Effects of removing residual culture medium, *J. Bacteriol.*, *173*(1), 197–203.

Thwaites, J. J., U. C. Surana, and A. M. Jones (1991), Mechanical properties of Bacillus subtilis cell walls—Effects of ions and lysozyme, *J. Bacteriol.*, *173*(1), 204–210.

Treves, D. S., B. Xia, J. Zhou, and J. M. Tiedje (2003), A two-species test of the hypothesis that spatial isolation influences microbial diversity in soil, *Microbial Ecol.*, *45*(1), 20–28.

Updegraff, D. M. (1982), Plugging and penetration of reservoir rock by microorganisms, paper presented at International Conference in Microbial Enhancement of Oil Recovery, U.S. Dept. of Energy, Bartlesville, Okla.

Vasseur, G., I. Djeranmaigre, D. Grunberger, G. Rousset, D. Tessier, and B. Velde (1995), Evolution of structural and physical parameters of clays during experimental compaction, *Mar. Petrol. Geol.*, *12*(8), 941–954.

Wellsbury, P., R. A. Herbert, and R. J. Parkes (1996), Bacterial activity and production in near-surface estuarine and freshwater sediments, *FEMS Microbiol. Ecol.*, *19*(3), 203–214.

Wellsbury, P., I. Mather, and R. J. Parkes (2002), Geomicrobiology of deep, low organic carbon sediments in the Woodlark Basin, Pacific Ocean, *FEMS Microbiol. Ecol.*, *42*(1), 59–70.

Yang, Y. L., and A. C. Aplin (1998), Influence of lithology and compaction on the pore size distribution and modelled permeability of some mudstones from the Norwegian margin, *Mar. Petrol. Geol.*, *15*(2), 163–175.

Yao, X., M. Jericho, D. Pink, and T. Beveridge (1999), Thickness and elasticity of gram-negative murein sacculi measured by atomic force microscopy, *J. Bacteriol.*, *181*(22), 6865–6875.

Zhang, C. L., A. V. Palumbo, T. J. Phelps, J. J. Beauchamp, F. J. Brockman, C. J. Murray, B. S. Parsons, and D. J. P. Swift (1998), Grain size and depth constraints on microbial variability in coastal plain subsurface sediments, *Geomicrobiol. J.*, *15*(3), 171–185.

Zhou, J. Z., B. C. Xia, D. S. Treves, L. Y. Wu, T. L. Marsh, R. V. O'Neill, A. V. Palumbo, and J. M. Tiedje (2002), Spatial and resource factors influencing high microbial diversity in soil, *Appl. Environ. Microbiol.*, *68*(1), 326–334.

Zhou, J. Z., B. C. Xia, H. Huang, A. V. Palumbo, and J. M. Tiedje (2004), Microbial diversity and heterogeneity in sandy subsurface soils, *Appl. Environ. Microbiol.*, *70*(3), 1723–1734.

Zweifel, U. L., and A. Hagstrom (1995), Total counts of marine-bacteria include a large fraction of non-nucleoid-containing bacteria (ghosts), *Appl. Environ. Microbiol.*, *61*(6), 2180–2185.